environments

Article

Water Purification and Electrochemical Oxidation: Meeting Different Targets with BDD and MMO Anodes

Monika R. Snowdon [1,*,†], Shasvat Rathod [1,*,†], Azar Fattahi [1], Abrar Khan [2], Leslie M. Bragg [3], Robert Liang [1], Norman Zhou [1] and Mark R. Servos [3]

[1] Centre for Advanced Materials Joining, Department of Mechanical and Mechatronics Engineering, University of Waterloo, Waterloo, ON N2L3G1, Canada
[2] Faculty of Arts and Science, Harvard University, Cambridge, MA 02138, USA
[3] Department of Biology, University of Waterloo, Waterloo, ON N2L3G1, Canada
* Correspondence: monika.snowdon@uwaterloo.ca (M.R.S.); shasvat.rathod@uwaterloo.ca (S.R.)
† These authors contributed equally to this work.

Abstract: The complex composition of natural organic matter (NOM) can affect drinking water treatment processes, leading to perceptible and undesired taste, color and odor, and bacterial growth. Further, current treatments tackling NOM can generate carcinogenic by-products. In contrast, promising substitutes such as electrochemical methods including electrooxidation (EO) have shown safer humic acid and algae degradation, but a formal comparison between EO methods has been lacking. In this study, we compared the Boron-doped diamond (BDD) electrode electrolysis performance for Suwannee River NOM degradation using mixed-metal oxide (MMO) anodes under different pH (6.5 and 8.5) representative of the high and low ranges for acidity and alkalinity in wastewater and applied two different current densities (10 and 20 mA cm^{-2}). BDD anodes were combined with either BDD cathodes or stainless steel (SS) cathodes. To characterize NOM, we used (a) total organic compound (TOC), (b) chemical oxygen demand (COD), (c) specific ultraviolet absorbance (SUVA), and (d) specific energy consumption. We observed that NOM degradation differed upon operative parameters on these two electrodes. BDD electrodes performed better than MMO under stronger current density and higher pH and proved to be more cost-effective. BDD-SS electrodes showed the lowest energy consumption at 4.4×10^3 kWh kg COD^{-1}. while obtaining a TOC removal of 40.2%, COD of 75.4% and SUVA of 3.4 at higher pH and current. On the contrary, MMO produced lower TOC, COD and SUVA at the lower pH. BDD electrodes can be used in surface water as a pre-treatment in combination with some other purification technologies to remove organic contaminants.

Keywords: electrochemical oxidation processes; boron doped diamond electrodes; mixed metal oxides anodes; Suwannee river NOM; water treatment

Citation: Snowdon, M.R.; Rathod, S.; Fattahi, A.; Khan, A.; Bragg, L.M.; Liang, R.; Zhou, N.; Servos, M.R. Water Purification and Electrochemical Oxidation: Meeting Different Targets with BDD and MMO Anodes. *Environments* **2022**, *9*, 135. https://doi.org/10.3390/environments9110135

Academic Editor: Simeone Chianese

Received: 15 August 2022
Accepted: 25 October 2022
Published: 27 October 2022

1. Introduction

The effectiveness of water treatment processes are affected by the presence and amount of natural organic matter (NOM) [1]. NOM, such as proteins, polysaccharides, aromatic and humic substances, promote unwanted taste, odor and bacterial growth which increase costs of water purification [2–5]. However, treatments to reduce NOM can trigger the development of carcinogenic or genotoxic disinfection by-products (DBP), specifically trihalomethanes and haloacetic acids, which are also undesired [2].

Currently, conventional NOM removal techniques include coagulation and flocculation, sedimentation, and filtration. Alternatively, newer techniques that use magnetic ion-exchange resins, activated carbon filters, and advanced oxidation processes (AOP) are more expensive [6–8]. Yet, these methods cannot eliminate all organic pollutants. Consequently, electrochemical AOP (EAOP) are regarded as promising in removing NOM. EAOP degrade organic matter via oxidation using hydroxyl radicals ($^{\cdot}OH$) that are produced at the anode-electrode surface. These radicals are non-selective and propagate a degradation

cycle with a broad variety of recalcitrant organic molecules [9]. Many different types of electrodes can be used in EAOP; some are conventional materials such as doped-SnO_2, PbO_2, and mixed metal oxides (MMO), while others are relatively newer options such as boron-doped diamond (BDD). The diamonds in BDD electrodes act as magnetic isolating materials, hence facilitating anodic oxidation in electrochemical water treatment [10]. The most common dopant for these electrodes is boron, which substitutes carbon atoms in the diamond crystal structure to promote a p-type semiconductor behaviour in the system [9,11]. BDD electrodes can be fabricated relatively inexpensively through chemical vapor deposition (CVD) and can degrade organic contaminants such as NH_3, C.N.-, phenol, organic dyes, surfactants, and landfill leachate [12–16]. In contrast, MMO electrodes are rarely made through CVD as it is difficult to introduce many metal precursors in the furnace [17]. MMO anodes have also been shown to have improved removal efficiency under high temperatures [18]. Yet, MMO electrodes are popular for wasterwater treatment due to their high resistance to corrosion and longevity, as well as operation at reduced electrolytic voltages. They are highly used for electrochlorinations, where the chlorine evolution reaction regarding MMOs has been summarized by Dong, Yu and Hoffmann [19].

As a reference, Table 1 provides a summary of published BDD studies for water purification. In these cases, electrodes allow for organic oxidation via two different mechanisms: (i) direct electron transfer (DET) using low applied potential, and (ii) indirect oxidation via $^{\bullet}OH$ formation [20]. In the DET mechanism, BDD anodes contain locations for the active adsorption of electrons and radicals, reducing the electrocatalytic activity of aliphatic -OHs, -COOHs, and secondary oxidations. With the indirect oxidation process, evidence shows that current densities increase at a potential over 2.3 V with -COOH concentrations [16,21]. BDD electrodes have low adsorption properties due to their inert surface, have a strong resistance to corrosion and have high overpotentials for oxygen evolution. Due to these characteristics, BDD electrolysis in the water discharge region can produce a high proportion of $^{\bullet}OH$ that are weakly adsorbed on the electrodes surface, creating an environment to propagate oxidation of organic molecules [22]. The equations below shows the reaction sequence where organic oxidation and oxygen evolution occur simultaneously [23]:

$$BDD + 2H_2O \rightarrow BDD(^{\bullet}OH) + 2H^+ + 2e^- \quad (1)$$

$$BDD(^{\bullet}OH) + R \rightarrow BDD + mCO_2 + nH_2O \quad (2)$$

If mineralization is incomplete, there will be some products formed from the reaction for Equation (2). In addition, organic evolution happens in competition with the $^{\bullet}OH$ terminating O_2 according to the following reaction [22]

$$BDD(^{\bullet}OH) \rightarrow BDD + \frac{1}{2}O_2 + H^+ + e^- \quad (3)$$

Evidence shows that secondary mechanisms are not occurring on the anode surface, where the development of $^{\bullet}OH$ takes place. Heard and Lennox detail the mechanisms at the MMO and BDD electrode interfaces [24].

Table 1. Electrochemical oxidation of different organic substances using a BDD anode.

Pollutant	Experimental Conditions	Average Efficiency	Refs.
Carboxylic Acids	i = 30 mA cm^{-2}; T = 30 °C; 1 M H_2SO_4	70–90%	[16,20,23]
Polyacrylates	i = 1–30 mA cm^{-2}; 1 M $HClO_4$	100%	[23]
Industrial wastewaters	i = 7–36 mA cm^{-2}; initial COD 1500–8000 mg L^{-1}	85–100%	[25]
Carwash wastewater	i = 15–60 mA cm^{-2}	40%	[26–28]
Wastewater from automotive industry	i = 30–50 mA cm^{-2}; initial COD 2500 mg L^{-1}	>90%	[29]

Although electrochemical techniques have been used as an alternative for NOM degradation, the control of the electrochemical reactions for NOM elimination has not been fully documented [8,25–30]. Because NOM includes a broad range of carbon compounds, insight-specific mechanisms have been typically inferred rather than explored in-depth. Other published works indicate that BDD electrodes are economically viable with conventional AOPs and dimensionally stable anodes (DSA), such as MMOs [31–34]; yet, no standard comparison between electrode materials exists with regard to NOM removal. Some studies have shown efficiencies of MMO and BDD, but the experimental conditions do not subject water samples to the same pH and current density. For example, Saha and colleagues performed a similar evaluation for cooling tower blowdown water under different flow rates and conductivities [35]. Other Recent work has shown a comparison between MMO and BDD anodes for winery wastewater for over 10 h at natural pH, demonstrating 85% mineralization with BDD due to the propensity for the system to generate more hydroxyl radicals [36]. In addition, a study on landfill leachate concluded Pt anodes outperformed BDD and MMO electrodes in terms of lower specific energy consumption and material cost [37]. However, a straightforward comparison using same pH and current density has been lacking. Therefore, our study assesses the performance of BDD and MMO electrodes during electrochemical oxidation (EO) of a standardized water matrix containing NOM under determined pH and currents. The water matrix was sourced from the Suwannee River, which is generally used as a reference according to the International Humic Substances Society [38]. Furthermore, we used a combination of total organic carbon (TOC), chemical oxygen demand (COD), and specific U.V. absorption (SUVA) as surrogate parameters to quantify NOM.

2. Materials and Methods

2.1. Reagents and Chemicals

To create the standard water matrix outlined by Rosenfeldt and Linden [39,40], we used $CaCl_2$, $MgCl_2{\cdot}6H_2O$, KNO_3, $CaSO_4{\cdot}2H_2O$, NaOH, $C_6H_{11}NO_6$, $NaHCO_3$, and Suwannee River NOM. Details are shown in Table 2. All reagents were acquired from Sigma-Aldrich (purity ≥99%). We analyzed two water matrices with pH = 6.5 and pH = 8.5. Table 3 shows the physico-chemical characteristics of the standardized water. Ultrapure water was used during all electrochemical experiments (18.2 MΩ.cm, 22 °C, Milli-Q® Advantage A10 Water Purification System, Merck KGaA, Darmstadt, Germany).

Table 2. Composition of standardized water matrix comprising Suwannee River NOM.

Compound	% *w*/*v*
$CaCl_2$	0.0226
$MgCl_2{\cdot}6H_2O$	0.0836
KNO_3	0.0041
$CaSO_4{\cdot}2H_2O$	0.0295
NaOH	0.0009
$NaHCO_3$	0.0126
$C_6H_{11}NO_6$	0.00258
Suwannee River NOM	0.0102

Table 3. Physico-chemical characteristics of the standardized water matrix.

Measurements	Units	Water Matrix 1	Water Matrix 2
pH	-	6.5	8.5
TOC	mg L^{-1}	6.25	7.03
UV_{254}	cm^{-1}	0.16	0.18
SUVA	L mg^{-1} m^{-1}	2.3	2.9

2.2. Electrochemical Setup

The experimental setup consisted of a batch system showing three electrode configurations: (i) BDD anode with a BDD cathode (BDD-BDD), (ii) BDD anode with stainless-steel cathode (BDD-SS), and (iii) MMO anode with stainless-steel cathode (MMO-SS). Titanium MMO and BDD anodes were purchased from William Gregor Ltd., East Grinstead, UK and Element Six, Didcot, UK. All electrodes had the same surface area (10 mm × 10 mm × 1 mm), and the gap between electrodes was 3 mm. Samples were square, roughly 1 cm in length and width; both sides were presumably active. The power supply was R-SPS605 60V DC Regulated manufactured by Nice Power, Southend-On-Sea, Essex, UK.

2.3. Electrochemical Degradation of Suwannee River NOM

Glass beakers with 300 mL of Suwannee River NOM water (pH = 6.5 or 8.5) were placed on the experimental setup, schematically illustrated in Figure 1. pH values were chosen to mimic natural water systems, using the two extremes at lower and higher natural alkalinity. A 30-min equilibration time was used at 400 rpm, followed by 30-, 60-, and 120 min. Each time point was organized as an individual experiment. A 0.45 µm polyethersulfone (PES) membrane filtered the treated water to eliminate particulate matter. Each treatment tested two different current densities (10 and 20 mA cm^{-2}). TOC, COD, and UV absorbance at 254 nm (UV254), taken at each time point, were used as substitute parameters to quantify NOM. TOC values were characterized with a Shimadzu© TOC-L analyzer with a Shimadzu ASI-L autosampler. We ran 4 iterations of every test and every test had 3 setups, and the PeCOD itself had 10 runs of every sample. There were 120 samples in total: 40 MMO-MMO, 40 BDD-SS, 40 MMO-SS.

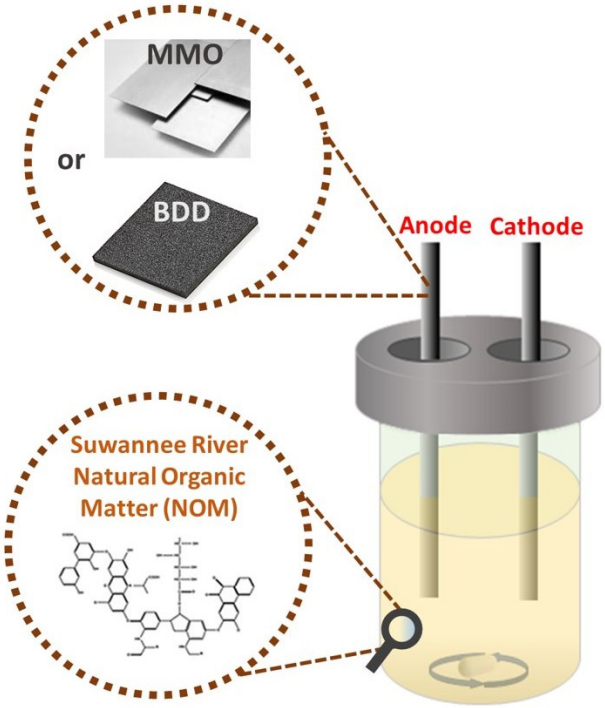

Figure 1. Schematic electrochemical setup containing BDD and MMO electrodes.

In particular, the apparatus used a 680 °C combustion catalytic oxidation detection method. MANTECH PeCOD© Analyzer was used to measure COD. UV254 values were determined via a fluorescence plate reader (spectral max M3, Molecular Devices) at 254 nm. The measurement occurs with shining UV light at a wavelength of 254 nm through an aqueous solution in a quartz cell to identify aromatics or unsaturated carbon bonds (alkenes, allenes) using the changes in the wavelength intensity [41]. TOC and COD elimination was

calculated using Equation (4), where C_0 and C_f were the initial and final organic carbon concentration and COD measured in mg L^{-1} [42]:

$$E_{TOC}\ (\%) = \frac{(C_0 - C_f)}{C_0} * 100\% \quad (4)$$

The SUVA was determined by normalizing the UV254 by dissolved organic carbon (DOC), using Equation (5):

$$SUVA = \frac{UV254}{DOC} \quad (5)$$

DOC represents the organic matter found after treatment of the sample with a 0.45 µm filter. The specific energy consumption per unit mass of COD (E_{sp} in kWh kg COD^{-1}) was determined using the subsequent Equation (6), adapted from [43–45]:

$$E_{sp} = \frac{10^3\ U \cdot I \cdot t}{(COD_0 - COD_f)V} \quad (6)$$

where U is the average electrolysis cell voltage (V), I is the applied electrolysis current (A), t is the electrolysis time (h), V is the synthetic water volume (L). The experiments were conducted at a water bath temperature of 22 °C. Temperature was not one of the parameters addressed in the study, however, with a current of 20 mA/cm^2 flowing between the electrodes, it cannot be ruled out that the solution can be heated by the current, through ohmic heating. The voltage applied varied in order to keep the current constant. Calculations are included in the Supplementary Information.

3. Results

3.1. TOC Removal

First, we examined the TOC removal. Figure 2 illustrates the TOC elimination at two pH levels (6.5, 8.5), in two separately applied current densities of 10 mA cm^{-2} and 20 mA cm^{-2}. The highest TOC elimination was observed for all treatment systems at 120 min; thus, this time point was used for quantitative comparisons (TOC removal over time for each treatment is illustrated in Figure S1). At pH 6.5 and 10 mA cm^{-2}, TOC elimination is amplified to 65.8% using MMO anodes and stainless-steel cathode (MMO-SS), whereas BDD-SS and BDD-BDD showed lower removals of −0.7% and 2.4%, respectively. Similarly, at 8.5 pH and 10 mA cm^{-2}, MMO-SS demonstrated peak TOC removal at 43.2%. In contrast, BDD-SS and BDD-BDD performed poorly at 8.8 and 1.9%, respectively (Figure 2).

Higher TOC removal at the lower current density (10 mA cm^{-2}) using MMO electrodes can account for their tendency for chlorine evolution. Cl^- ions in the water matrix can affect the EO. One such effect is the competition of these Cl^- ions with organic contaminants for active sites on the electrode surface or free radicals in the solution, thereby decreasing the NOM degradation rate [46–48]. Additionally, low current densities have resulted in fairly low removal percentages in previous studies [31,32,34,49].

Subsequently, as shown in Figure 2, bringing up the current density to 20 mA cm^{-2} strongly influenced organic matter oxidation. At 6.5 pH and 20 mA cm^{-2}, BDD-BDD revealed the most significant removal growth, flatlined at 52.8%. MMO-SS removal was reduced to 14%, and BDD-SS demonstrated a TOC elimination of 1.2%. At a 6.5 pH, raising the current density had varied results with BDD anodes. On the contrary, at pH 8.5, BDD-BDD and BDD-SS produced the most significant TOC elimination at 40.2, 40.1, and 34.9% for MMO-SS, respectively. Increased pH has been observed to enhance the incidence of oxygen evolution; so, more oxidative species were produced in the aqueous solution, which increased NOM degradation in BDD anodes. Increasing the current density to 20 mA cm^{-2} in turn also improved the TOC elimination and prevented the primary increase in partial oxidated carbon chains in the TOC characterization.

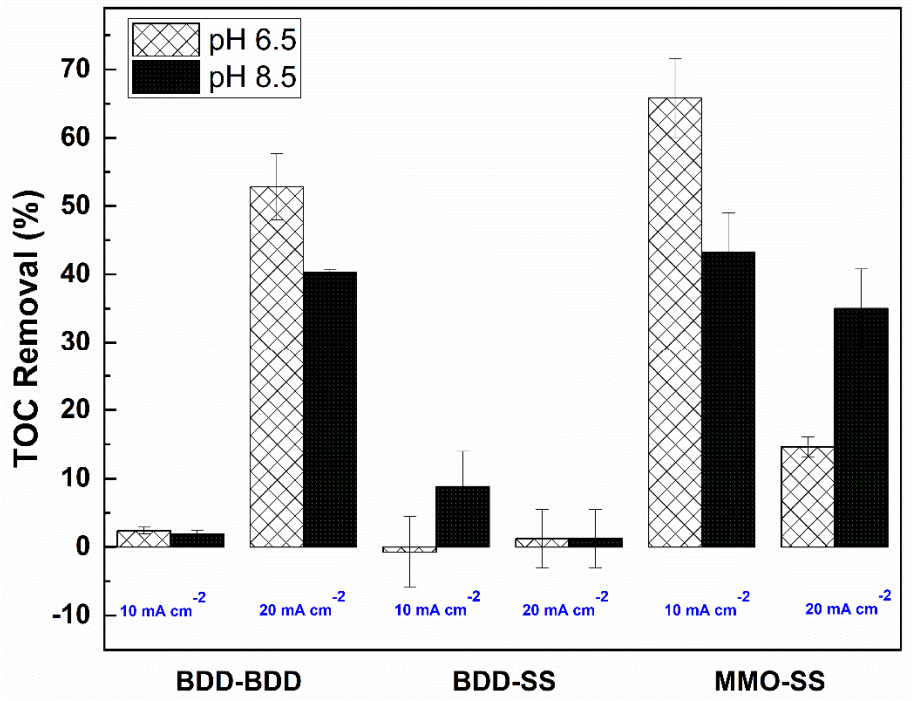

Figure 2. TOC removal after 120 min EO treatment with BDD and MMO anodes at pH 6.5 and 8.5 and current densities of 10 and 20 mA cm^{-2}. Error bars show standard deviation.

Additionally, the TOC removal in this study was higher than in AOP systems alone. Fattahi et al. (2021). attained a removal efficiency of only 30% with TiO_2 photocatalysis irradiated by UV254 [50]. However, other studies using EAOP systems with higher current densities reported higher TOC removal. For instance, Gandini et al. (2013) and Chen et al. (2000) stated a removal capacity of 81% with a Ti-BDD anode using 38 mA cm^{-2} [20,51].

3.2. COD Removal

COD measures the oxygen equivalent of the organic matter in an aqueous sample that is prone to oxidation when the water is exposed to a strong chemical oxidant. Its removal pattern is different from that of TOC. However, like the TOC measurement, the longest electrolysis interval at 120 min established the most effective COD removal (Figure S2). At pH = 6.5 and 10 mA cm^{-2}, MMO-SS displayed the maximum COD elimination at 91.6%., whereas BDD-SS and BDD-BDD had decreased COD elimination at 3.8 and −17.7%, respectively (Figure 3). The increase in COD removal for BDD-BDD electrodes at 120 min can be related to the agglomerates produced in the mixture, which boosted the floc size of the NOM. COD equipment used to test the samples was unsuccessful in recognizing the larger flocs, which may have affected the overall COD results.

At pH 8.5 and 10 mA cm^{-2}, BDD-SS and BDD-BDD showed an increase in COD removal of 52.8 and 43.8%. The BDD electrodes do not appear to substantially differentiate COD removal over MMO electrodes at the lower current and the higher pH (8.5) settings. Although COD efficiency was decreased in the case of the BDD-SS and BDD-BDD electrodes at the higher pH than with the MMO-SS electrodes, it was still more effective than TOC efficiency removal with the same parameters.

At pH 6.5 and 20 mA cm^{-2}, the COD elimination increased to 52.2 and 63.2% for BDD-SS and BDD-BDD, respectively (Figure 3). Nonetheless, MMO-SS accomplished the highest COD removal at 90.2%. Alternatively, at pH 8.5 and 20 mA cm^{-2}, BDD-SS and BDD-BDD demonstrated COD elimination at 75.4 and 57.6%, respectively. MMO-SS decreased in COD removal at higher pH to 68.8%. Thus, MMO electrode demonstrated a greater removal at pH 6.5 for all current densities; though, BDD electrode efficiencies were enhanced at pH 8.5 and the stronger current density.

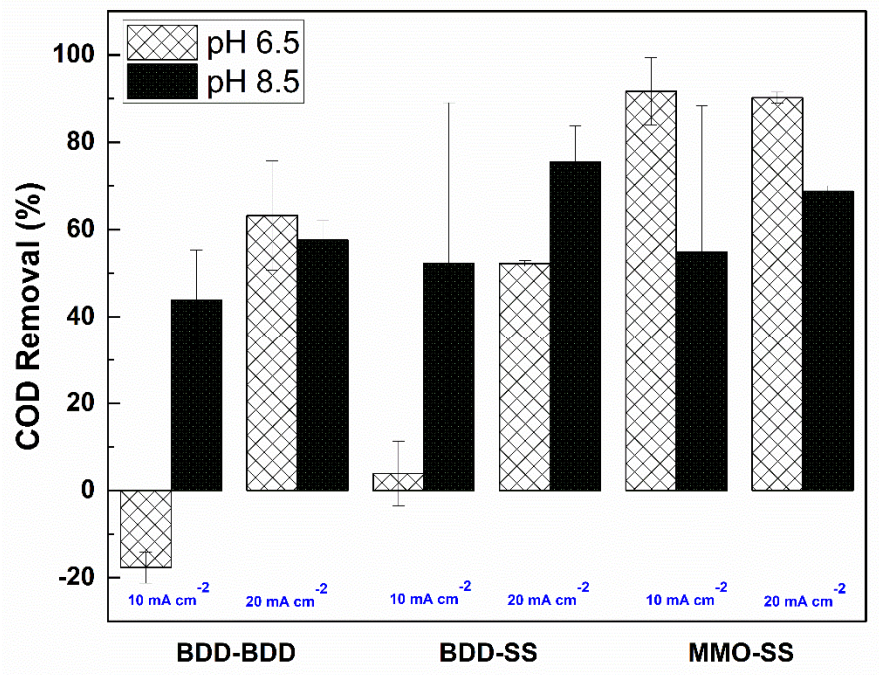

Figure 3. COD removal after 120 min after EO treatment with BDD and MMO electrodes at pH 6.5 and 8.5 and current densities of 10 and 20 mA cm^{-2}. Error bars show standard deviation.

MMO and BDD efficiencies may be due to separate reaction pathways occurring between the non-active (BDD) and active (MMO) electrodes. BDD is known as a 'non-active' anode since it does not offer a catalytically active site for reactant adsorption in aqueous solutions. Instead, the $^{\cdot}OH$ that forms through water discharge reactions on the anode surface is responsible for electrochemical degradation of organic compounds. In contrast, MMO is an 'active' anode with low oxygen evolution overpotential [52,53]. $^{\cdot}OH$ can be produced through the following reactions:

$$MO_x + H_2O \rightarrow MO_x(^{\cdot}OH) + H^+ \quad (7)$$

$$MO_x(^{\cdot}OH) \rightarrow MO_{x+1} + H^+ + e^- \quad (8)$$

$$MO_{x+1} + R \rightarrow MO_x + RO \quad (9)$$

MO_{x+1} are active species on the electrode and react with organics (R) in the solution [34]. However, MMO electrodes have high electrocatalytic activity for chlorine evolution. Thus, active chlorines such as HClO and Cl_2 form through indirect oxidation of Cl^- according to the reactions below [50]:

$$Cl^- \leftrightarrow Cl_{ads} + e^- \quad (10)$$

$$Cl_{ads} + Cl^- \leftrightarrow Cl_2 + e^- \quad (11)$$

$$Cl_2 + H_2O \leftrightarrow HClO + H^+ + Cl^- \quad (12)$$

Different reaction mechanisms can also cause differences in COD and TOC removals. MO_x and MO_{x+1} may affect TOC removal. Moreover, low pH favored MMO anodic oxidation by forming Cl^- ions that were propagated by the current density. The Cl^- assists in organic oxidation by route of active chlorine at approximately pH 6.5 [49]. Increasing pH lowered the concentration of Cl^- in the solution; therefore, we observed that the hydroxide radicals generated higher TOC removal via BDD anodes. This reaction displayed weak adsorption properties of the BDD anode and a large generation of $^{\cdot}OH$ thus increasing TOC removal over COD removal [49].

The theoretical oxygen demand (ThoD) was compared with the obtained COD using a MANTECH COD analyzer, ThoD was calculated using Equation (13) formulated by Baker et al. centered on a wide range of organic acids and Suwannee river NOM components [54]:

$$C_n H_m O_c X_k N_j S_i P_h + bO_2 \rightarrow nCO_2 + \frac{m - k - 3j - 2i - 3h}{2} H_2O + kHX + jNH_3 + iH_2SO_4 \quad (13)$$

where X is the sum of halogens, and b is the oxygen demand calculated using Equation (14):

$$b = n + \frac{m - k - 3j - 2i - 3h}{4} - \frac{e}{2} + 2i + 2h \quad (14)$$

In Table 4, the photoelectro chemical oxygen demand (PeCOD) measurement was only 15% lower than theoretical values, demonstrating that the PeCOD can be used as a predictor of ThOD for the molecules in the synthesized water mixture.

Table 4. Evaluation of synthetic NOM matrix ThOD to PeCOD measurement.

	Oxygen Demand [mg L^{-1}]
Theoretical Calculation	21.21
PeCOD measurement	18

In addition, Stoddart et al. [55] identified a metric of NOM quantification as COD/TOC ratio, which measures the degree of reduction of the organic compounds. A higher COD/TOC ratio indicates high degradation by-products and, therefore, NOM reduction [55,56]. This ratio is a direct measure of the average oxidation state of a carbon in the wastewater sample. The ranges for this ratio are from zero to 5.33, where the higher the value, the higher the impact of the NOM molecules on the concentration of the surface water oxygen. Lower numbers are therefore desirable. Table 5 shows COD/TOC ratios at 120 min of treatment. A full table of summarized data is available in the Supplemental Materials (Table S1). At the lower pH and lower current settings (pH = 6.5 and 10 mA cm^{-2}), MMO-SS demonstrated the lowest NOM content, meaning that MMO electrodes perform better in contrast to the BDD anode setups at low pH and low current. At the higher pH of 8.5 and lower current settings, BDD-SS and MMO-SS showed the lowest COD/TOC ratio at 0.66 and 0.68. In contrast, BDD-BDD showed a higher COD/TOC ratio of 1.01. These results exposed a better electrochemical performance at pH 8.5. Further, at lower pH and higher current settings (6.5 pH, 20 mA cm^{-2}), COD/TOC ratios were higher in BDD-BDD electrodes, compared to BDD-SS and MMO-SS, reaching a value of 0.77 and 0.55 and 0.45, respectively. However, there was no substantial difference between BDD-SS and MMO-SS electrodes at high and low pH, meaning the electrochemical performance of electrodes at high current densities was unaffected by pH variation based on COD/TOC ratio [34,57–59]. The standard error is large for the MMO anodes, even with many iterations of the measurements at the low current. This observation could be due to a leak that caused the anodes to oxidize on the backside that is not corrosion resistant.

Table 5. COD/TOC ratio for different electrode configurations, pH and current densities.

Electrodes	**Current Density = 10 mA cm^{-2}**		**Current Density = 20 mA cm^{-2}**	
	pH = 6.5	**pH = 8.5**	**pH = 6.5**	**pH = 8.5**
BDD-BDD	1.3 ± 0.7	1.01 ± 0.4	0.77 ± 0.07	0.73 ± 0.1
BDD-SS	1.74 ± 0.7	0.67 ± 0.4	0.55 ± 0.4	0.57 ± 0.2
MMO-SS	0.33 ± 0.3	0.67 ± 0.6	0.45 ± 0.1	0.59 ± 0.1

3.3. Specific UV Absorbance

UV254 quantifies NOM in water because aromatics have greater absorbance at 254 nm. For instance, UV254 is normalized to DOC to give the SUVA, which is an indicator of

aromaticity (Equation (5)). Previous studies indicated that the presence of a high TOC, color, and SUVA in drinking water increased the likelihood of disinfection by-products such as trihalomethanes (THMs) and haloacetic acids (HAAs) being present in the purified solution. THMs and HAAs are products of the electro-generation active chlorines. However, the oxidization of Cl^- at the MMO anode to chlorine, which hydrolyzes into hypochlorous acids (Equations (13)–(15)), leading to the electro chlorination of carbon molecules in the mixture [53].

The standard SUVA value for the synthesized aqueous solution was 2.5 L mg^{-1} m^{-1} indicating that the NOM moieties present were more hydrophilic and had a lower molecular weight [2,60–63]. However, after 120 min of electrochemical treatment, SUVA increased, indicating an improvement in UV_{254} absorbing species, as in, for instance, aromatic molecules (Figure 4). While SUVA increased as the purification process progressed, TOC and DOC declined, as revealed by the total TOC reduction (Figure 2). Consequently, the organics present in the synthetic water decreased, but the residual organic matter increased to a higher ratio of aromatic character than in the original state. Earlier experiments established that an increase in aromaticity does not correlate with increased humic substances [64] but they are an indicator for aromatic character and provide a general relation to the development of disinfection by-products.

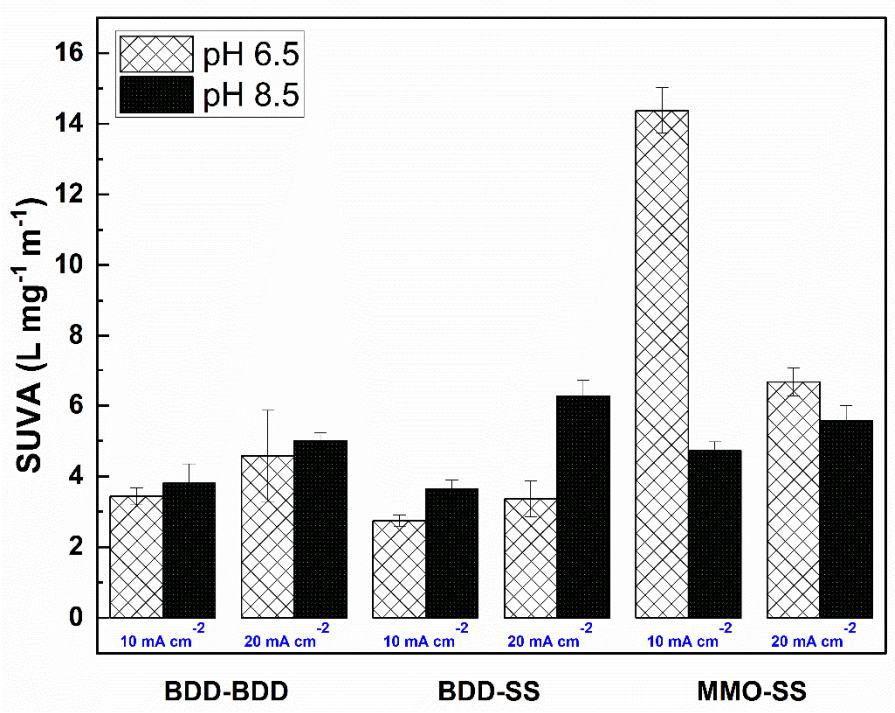

Figure 4. SUVA values of Suwannee River NOM after 120 min treatment using BDD and MMO electrodes at pH = 6.5 and 8.5 and current densities of 10 and 20 mA cm^{-2}. Error bars show standard deviation.

At pH 6.5, 10 mA cm^{-2}: the SUVA was highest for MMO-SS at 14.4. BDD-BDD and BDD-SS were considerably lower at 3.4 and 2.7. However, at 8.5 pH, SUVA was reduced for the MMO-SS system to 4.7, while the other electrode sets remained near their 6.5 pH values, at 3.8 and 3.6, respectively. Hence, BDD electrodes have a higher resistance to pH changes in the standard aqueous NOM mixture.

At 6.5 pH, 20 mA cm^{-2}: the SUVA values were 4.6, 3.4, and 6.7 for BDD-BDD, BDD-SS, and MMO-SS, respectively. In contrast, at 8.5 pH and 20 mA cm^{-2}, SUVA improved for all systems to 5, 6.3, and 5.6, respectively, for the BDD-BDD, BDD-SS, and MMO-SS systems. The performance of BDD electrodes increased at higher current and pH. MMO electrodes, however, were adversely affected by increases in current and pH.

It is relevant to point that at a higher pH and higher current, there were more agglomerations visible in the MMO-SS system, shown by more yellow particulates and prominent water discoloration. The Ti present in the MMO anode introduced metallic coagulants to the electrochemical treatment, which increased the synthetic NOM floc (size, strength, structure, and recovery potential). However, due to the lack of agglomeration in BDD electrode systems, they showed lower SUVA.

3.4. Estimation of Specific Energy Consumption

Figure 5 represents the specific energy consumption of the samples calculated using Eqn. 6. Determined at the lower applied current density, BDD-SS was examined to have the lowest energy consumption at 1.5×10^3 kWh kg COD^{-1} at pH = 8.5. At 20 mA cm^{-2}, BDD-SS electrodes showed the lower specific energy consumption at 4.4×10^3 kWh kg COD^{-1} when tested at the higher pH. Therefore, BDD anodes augment the current input for the EO process at low and high current densities in the presence of higher pH. However, increasing high current densities would increase charge passed (Ah dm^{-3}) using BDD-SS electrodes [37]. The same conclusion was reported by Zhou et al. (2011), comparing methyl orange degradation using EO on two electrodes BDD and MMO. Their results demonstrated that BDD electrodes have higher general current efficiency than those of MMO [34]. The observations here also correlate well with recent results where BBD has a higher removal efficiency than MMO over a wider range of conditions. Generally, electrolysis performance is better under acidic conditions. Both BDD and MMO anodes could perform better under acidic conditions [65–67] and performance will likely decrease above a pH of 8.5, in particular, as we have observed here for the MMO-SS electrode system. However, it seems BDD is more consistent in performance and will perform better than MMO at pH extremes.

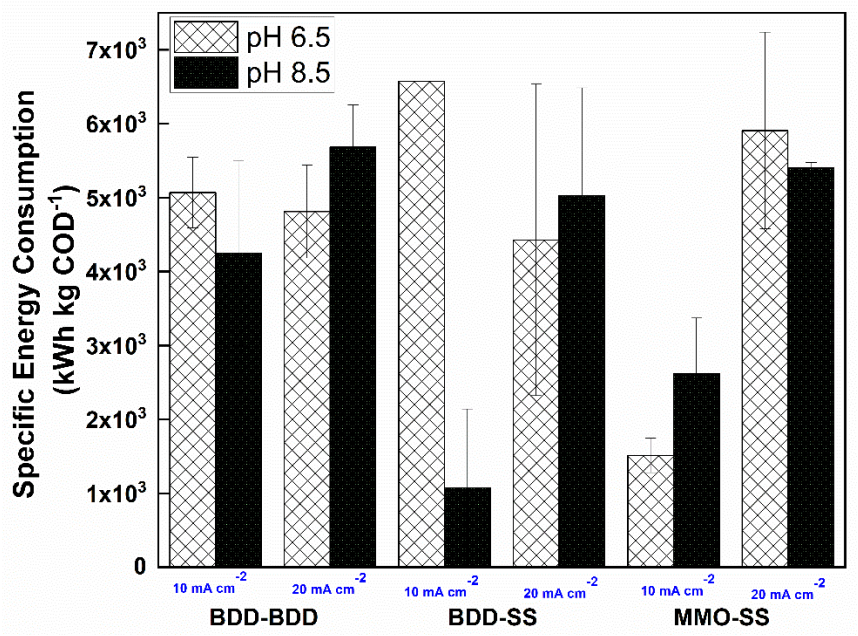

Figure 5. Specific energy consumption of BDD and MMO electrodes at pH 6.5 and 8.5, and current densities of 10 and 20 mA cm^{-2}. Error bars showcase the standard deviation.

4. Conclusions

Electrochemical oxidation of standardized Suwannee River NOM was examined using BDD and MMO electrodes at two different current densities (10 and 20 mA cm^{-2}) and pH (6.5 and 8.5). We identified that the electrooxidation via BDD and MMO anodes was significantly dependent on the current density. We observed that the BDD electrodes displayed higher removal of NOM in the presence of the higher current density. The highest TOC and COD removal were observed with MMO electrodes at a pH of

6.5 (10 mA cm^{-2}) where TOC was 65.8%, COD was 91.6%, and the SUVA peaked at 14.4. The BDD-BDD electrodes had the highest TOC of 52.8% and COD of 63.2% with a SUVA of 4.6 when treated with a pH of 6.5 at 20 mA cm^{-2}, whereas BDD-SS observed its highest TOC removal of 40.2% and DOC of 75.4% with a SUVA of 3.4 when the conditions where a pH of 8.5 at 20 mA cm^{-2}. Initial pH did not profoundly affect NOM oxidation.

Overall, through this comparative analysis, we observed that the MMO electrode system exhibit improved performance at pH 6.5 and lower current (10 mA cm^{-2}) from 0–30 min. MMO electrodes were more effective than BDD for COD and TOC elimination at the lower current density. However, more importantly, the removal efficiency of the BDD electrodes demonstrated a higher oxidation of the NOM under a broader range of operating conditions (duration, current, pH). To add, BDD-based electrodes had the lowest energy consumption and outperformed MMO electrodes at both the higher pH and current studied. These observations reaffirm BDD's utility, being a low capacitance material and electrochemically stable. Moreover, SUVA data showcased a more effective breakdown of NOM with BDD electrodes. Future experiments applying higher current densities can help to establish the commercialization of BDD anodes for the removal of NOM from water sources.

Supplementary Materials: The following supporting information can be downloaded at: https://www.mdpi.com/article/10.3390/environments9110135/s1, Figure S1. TOC Removal using BDD-BDD, BDD-SS, and MMO-SS electrode setups. (a) pH 6.5; current density: 10 mA cm^{-2} (b) pH 6.5; current density: 20 mA cm^{-2} (c) pH 8.5; current density: 10 mA cm^{-2} (d) pH 8.5; current density: 20 mA cm^{-2}; Figure S2. COD removal COD using BDD-BDD, BDD-SS, and MMO-SS electrode setups. (a) pH 6.5; current density: 10 mA cm^{-2} (b) pH 6.5; current density: 20 mA cm^{-2} (c) pH 8.5; current density: 10 mA cm^{-2} (d) pH 8.5; current density: 20 mA cm^{-2}. Table S1. Summary of TOC and COD removal results for each electrode configuration and the two pHs. Excel with calculations and raw data.

Author Contributions: Conceptualization, R.L. and M.R.S. (Monika R. Snowdon); methodology, R.L.; software, A.F., M.R.S. (Monika R. Snowdon) and S.R.; validation, S.R, L.M.B. and A.K.; formal analysis, S.R., M.R.S. (Monika R. Snowdon) and A.F.; investigation, S.R.; resources, S.R.; data curation S.R.; writing—original draft preparation, S.R., M.R.S. (Monika R. Snowdon) and A.F.; writing—review and editing, S.R., M.R.S. (Monika R. Snowdon), R.L. and A.F.; visualization, S.R.; supervision, R.L., M.R.S. (Monika R. Snowdon), N.Z. and M.R.S. (Mark R. Servos); project administration, R.L. funding acquisition, R.L. All authors have read and agreed to the published version of the manuscript.

Funding: This work was supported by the Canada Research Chair (CRC) in water quality protection and advanced materials joining and processing, Natural Sciences and Engineering Research Council (NSERC) of Canada; Strategic Project Grant (STPGP 430654-12). Furthermore, the authors would like to acknowledge the assistance provided by the Schwartz-Reisman Foundation under the Waterloo-Technion Research Co-operation Program.

Data Availability Statement: Excel with raw data and calculations is available as part of the Supplemental Materials. All other datasets generated during and/or analyzed during the current study are available from the corresponding authors on reasonable request.

Acknowledgments: The authors would like to thank the full-time staff and members of the Servos lab, in particular Leslie M. Bragg, and the Centre of Advanced Materials joining for their insight and assistance on the project.

Conflicts of Interest: The authors declare no conflict of interest.

References

1. Goslan, E.H.; Fearing, D.A.; Banks, J.; Wilson, D.; Hills, P.; Campbell, A.T.; Parsons, S.A. Seasonal variations in the disinfection by-product precursor profile of a reservoir water. *J. Water Supply Res. Technol. AQUA* **2002**, *51*, 475–482. [CrossRef]
2. Ates, N.; Kitis, M.; Yetis, U. Formation of chlorination by-products in waters with low SUVA-correlations with SUVA and differential UV spectroscopy. *Water Res.* **2007**, *41*, 4139–4148. [CrossRef] [PubMed]
3. Jarusutthirak, C.; Amy, G.; Croué, J.P. Fouling characteristics of wastewater effluent organic matter (EfOM) isolates on NF and UF membranes. *Desalination* **2002**, *145*, 247–255. [CrossRef]

4. Chowdhury, S.; Champagne, P.; McLellan, P.J. Models for predicting disinfection by-product (DBP) formation in drinking waters: A chronological review. *Sci. Total Environ.* **2009**, *407*, 4189–4206. [CrossRef] [PubMed]
5. Snowdon, M.; Liang, R.; Leeuwen, J.C.V.; Schneider, O.; Khan, A.; Fong, L.C.M.L.C.; Zhou, N.Y.; Servos, M.R. Pharmaceutical Micropollutant Treatment with UV–LED/TiO_2 Photocatalysis under Various Lighting and Matrix Conditions. *Photochem* **2022**, *2*, 503–514. [CrossRef]
6. Wang, G.; Zhang, L.; Zhang, J. A review of electrode materials for electrochemical supercapacitors. *Chem. Soc. Rev.* **2012**, *41*, 797–828. [CrossRef] [PubMed]
7. Kim, H.C.; Yu, M.J. Characterization of natural organic matter in conventional water treatment processes for selection of treatment processes focused on DBPs control. *Water Res.* **2005**, *39*, 4779–4789. [CrossRef]
8. MikaSillanpää, M.; Matilainen, A.; Lahtinen, T. Chapter 2—Characterization of NOM. In *Natural Organic Matter in Water*; Elsevier: Amsterdam, The Netherlands, 2015; pp. 17–45. [CrossRef]
9. Chaplin, B.P. Critical review of electrochemical advanced oxidation processes for water treatment applications. *Environ. Sci. Process. Impacts* **2014**, *16*, 1182–1203. [CrossRef] [PubMed]
10. Suffredini, H.B.; Machado, S.A.S.; Avaca, L.A. The water decomposition reactions on boron-doped diamond electrodes. *J. Braz. Chem. Soc.* **2004**, *15*, 16–21. [CrossRef]
11. Perret, A.; Haenni, W.; Skinner, N.; Tang, X.M.; Gandini, D.; Comninellis, C.; Correa, B.; Foti, G. Electrochemical behavior of synthetic diamond thin film electrodes. *Diam. Relat. Mater.* **1999**, *8*, 820–823. [CrossRef]
12. Chen, X.; Chen, G.; Yue, P.L. Anodic oxidation of dyes at novel Ti/B-diamond electrodes. *Chem. Eng. Sci.* **2003**, *58*, 995–1001. [CrossRef]
13. Lai, C.L.; Lin, S.H. Treatment of chemical mechanical polishing wastewater by electrocoagulation: System performances and sludge settling characteristics. *Chemosphere* **2004**, *54*, 235–242. [CrossRef] [PubMed]
14. Iniesta, J.; Michaud, P.A.; Panizza, M.; Comninellis, C.H. Electrochemical oxidation of 3-methylpyridine at a boron-doped diamond electrode: Application to electroorganic synthesis and wastewater treatment. *Electrochem. Commun.* **2001**, *3*, 346–351. [CrossRef]
15. Tenne, R.; Patel, K.; Hashimoto, K.; Fujishima, A. Efficient electrochemical reduction of nitrate to ammonia using conductive diamond film electrodes. *J. Electroanal. Chem.* **1993**, *347*, 409–415. [CrossRef]
16. Chen, G. Electrochemical technologies in wastewater treatment. *Sep. Purif. Technol.* **2004**, *38*, 11–41. [CrossRef]
17. Wu, W.; Huang, Z.H.; Lim, T.T. Recent development of mixed metal oxide anodes for electrochemical oxidation of organic pollutants in water. *Appl. Catal. A Gen.* **2014**, *480*, 58–78. [CrossRef]
18. Scialdone, O.; Galia, A.; Randazzo, S. Oxidation of carboxylic acids in water at IrO_2–Ta_2O_5 and boron doped diamond anodes. *Chem. Eng. J.* **2011**, *174*, 266–274. [CrossRef]
19. Dong, H.; Yu, W.; Hoffman, M.R. Mixed Metal Oxide Electrodes and the Chlorine Evolution Reaction. *J. Phys. Chem. C* **2021**, *125*, 20745–20761. [CrossRef]
20. Gandini, D.; Mahé, E.; Michaud, P.A.; Haenni, W.; Perret, A.; Comninellis, C. Oxidation of carboxylic acids at boron-doped diamond electrodes for wastewater treatment. *J. Appl. Electrochem.* **2000**, *30*, 1345–1350. [CrossRef]
21. Cañizares, P.; García-Gómez, J.; Lobato, J.; Rodrigo, M.A. Electrochemical oxidation of aqueous carboxylic acid wastes using diamond thin-film electrodes. *Ind. Eng. Chem. Res.* **2003**, *42*, 956–962. [CrossRef]
22. da Silva, S.W.; Navarro, E.M.O.; Rodrigues, M.A.S.; Bernardes, A.M.; Perez-Herranz, V. Using p-Si/BDD anode for the electrochemical oxidation of norfloxacin. *J. Electroanal. Chem.* **2019**, *832*, 112–120. [CrossRef]
23. Marselli, B.; Garcia-Gomez, J.; Michaud, P.-A.; Rodrigo, M.A.; Comninellis, C. Electrogeneration of Hydroxyl Radicals on Boron-Doped Diamond Electrodes. *J. Electrochem. Soc.* **2003**, *150*, D79. [CrossRef]
24. Heard, D.M.; Lennox, A.J.J. Electrode Materials in Modern Organic Electrochemistry. *Angew. Chem.* **2020**, *59*, 18866–18884. [CrossRef]
25. Ben-Sasson, M.; Zidon, Y.; Calvo, R.; Adin, A. Enhanced removal of natural organic matter by hybrid process of electrocoagulation and dead-end microfiltration. *Chem. Eng. J.* **2013**, *232*, 338–345. [CrossRef]
26. Bagga, A.; Chellam, S.; Clifford, D.A. Evaluation of iron chemical coagulation and electrocoagulation pretreatment for surface water microfiltration. *J. Membr. Sci.* **2008**, *309*, 82–93. [CrossRef]
27. Gamage, N.P.; Chellam, S. Mechanisms of physically irreversible fouling during surface water microfiltration and mitigation by aluminum electroflotation pretreatment. *Environ. Sci. Technol.* **2014**, *48*, 1148–1157. [CrossRef]
28. Chellam, S.; Sari, M.A. Aluminum electrocoagulation as pretreatment during microfiltration of surface water containing NOM: A review of fouling, NOM, DBP, and virus control. *J. Hazard. Mater.* **2016**, *304*, 490–501. [CrossRef]
29. Ødegaard, H.; Østerhus, S.; Melin, E.; Eikebrokk, B. NOM removal technologies—Norwegian experiences. *Drink. Water Eng. Sci.* **2010**, *3*, 1–9. [CrossRef]
30. Matilainen, A.; Gjessing, E.T.; Lahtinen, T.; Hed, L.; Bhatnagar, A.; Sillanpää, M. An overview of the methods used in the characterisation of natural organic matter (NOM) in relation to drinking water treatment. *Chemosphere* **2011**, *83*, 1431–1442. [CrossRef]
31. Sillanpää, M.; Särkkä, H.; Vepsäläinen, M. NOM Removal by Electrochemical Methods. In *Natural Organic Matter in Water: Characterization and Treatment Methods*; Elsevier: Amsterdam, The Netherlands, 2015; ISBN 9780128017197.

32. Soni, B.D.; Patel, U.D.; Agrawal, A.; Ruparelia, J.P. Application of BDD and DSA electrodes for the removal of RB 5 in batch and continuous operation. *J. Water Process Eng.* **2017**, *17*, 11–21. [CrossRef]
33. Zhou, M.; Liu, L.; Jiao, Y.; Wang, Q.; Tan, Q. Treatment of high-salinity reverse osmosis concentrate by electrochemical oxidation on BDD and DSA electrodes. *Desalination* **2011**, *277*, 201–206. [CrossRef]
34. Zhou, M.; Särkkä, H.; Sillanpää, M. A comparative experimental study on methyl orange degradation by electrochemical oxidation on BDD and MMO electrodes. *Sep. Purif. Technol.* **2011**, *78*, 290–297. [CrossRef]
35. Saha, P.; Bruning, H.; Wagner, T.V.; Rijnaarts, H.H.M. Removal of organic compounds from cooling tower blowdown by electrochemical oxidation: Role of electrodes and operational parameters. *Chemosphere* **2020**, *259*, 127491. [CrossRef] [PubMed]
36. Lauzurique, Y.; Espinoza, L.C.; Huiliñir, C.; García, V.; Salazar, R. Anodic Oxidation of Industrial Winery Wastewater Using Different Anodes. *Water* **2022**, *14*, 95. [CrossRef]
37. Can, O.T.; Gazigil, L.; Keyikoglu, R. Treatment of intermediate landfill leachate using different anode materials in electrooxidation process. *Environ. Prog. Sustain. Energy* **2022**, *41*, e13722. [CrossRef]
38. Green, N.W.; McInnis, D.; Hertkorn, N.; Maurice, P.A.; Perdue, E.M. Suwannee River natural organic matter: Isolation of the 2R101N reference sample by reverse osmosis. *Environ. Eng. Sci.* **2015**, *32*, 38–44. [CrossRef]
39. Rosenfeldt, E.J.; Linden, K.G. Degradation of endocrine disrupting chemicals bisphenol A, ethinyl estradiol, and estradiol during UV photolysis and advanced oxidation processes. *Environ. Sci. Technol.* **2004**, *38*, 5476–5483. [CrossRef]
40. Rosenfeldt, E.J.; Chen, P.J.; Kullman, S.; Linden, K.G. Destruction of estrogenic activity in water using UV advanced oxidation. *Sci. Total Environ.* **2007**, *377*, 105–113. [CrossRef]
41. SpectraMax M Series Microplate Readers, The Ultimate Guide to Microplate Reader Solutions (eBook). Available online: https://www.moleculardevices.com/en/assets/ebook/br/ultimate-guide-to-microplate-reader-solutions (accessed on 26 August 2022).
42. Manea, F.; Jakab, A.; Ardelean, M.; Pop, A.; Vlaicu, I. Boron-doped diamond electrode-based advanced treatment methods for drinking water. *Environ. Eng. Manag. J.* **2014**, *13*, 2167–2172. [CrossRef]
43. Pétrier, C. The use of power ultrasound for water treatment. In *Power Ultrasonics*; Gallego-Juárez, J.A., Graff, K.F., Eds.; Woodhead Publishing: Oxford, UK, 2015; p. 953.
44. Stefan, M.I. (Ed.) Chapter 2 UV/Hydrogen Peroxide Process. In *Advanced Oxidation Processes for Water Treatment: Fundamentals and Applications*; IWA Publishing: London, UK, 2017; pp. 50–52.
45. Huang, K.L.; Liu, C.C.; Ma, C.Y.; Chen, T.T. Effects of operating parameters on electrochemical treatment of swine wastewater. *Int. J. Electrochem. Sci.* **2019**, *14*, 11325–11339. [CrossRef]
46. Wiszniowski, J.; Robert, D.; Surmacz-Gorska, J.; Miksch, K.; Weber, J.-V. Photocatalytic mineralization of humic acids with TiO2: Effect of pH, sulfate and chloride anions. *Int. J. Photoenergy* **2003**, *5*, 69–74. [CrossRef]
47. Piscopo, A.; Robert, D.; Weber, J.V. Influence of pH and chloride anion on the photocatalytic degradation of organic compounds: Part I. Effect on the benzamide and para-hydroxybenzoic acid in TiO_2 aqueous solution. *Appl. Catal. B Environ.* **2001**, *35*, 117–124. [CrossRef]
48. Abdullah, M.; Low, G.K.C.; Matthews, R.W. Effects of common inorganic anions on rates of photocatalytic oxidation of organic carbon over illuminated titanium dioxide. *J. Phys. Chem.* **1990**, *94*, 6820–6825. [CrossRef]
49. da Silva, A.J.C.; dos Santos, E.V.; de Oliveira Morais, C.C.; Martínez-Huitle, C.A.; Castro, S.S.L. Electrochemical treatment of fresh, brine and saline produced water generated by petrochemical industry using Ti/IrO_2-Ta_2O_5 and BDD in flow reactor. *Chem. Eng. J.* **2013**, *233*, 47–55. [CrossRef]
50. Fattahi, A.; Arlos, M.J.; Bragg, L.M.; Liang, R.; Zhou, N.; Servos, M.R. Degradation of natural organic matter using Ag-P25 photocatalyst under continuous and periodic irradiation of 405 and 365 nm UV-LEDs. *J. Environ. Chem. Eng.* **2021**, *9*, 104844. [CrossRef]
51. Clematis, D.; Klidi, N.; Barbucci, A.; Carpanese, M.P.; Delucchi, M.; Cerisola, G.; Panizza, M. Application of electro-fenton process for the treatment of methylene blue. *Bulg. Chem. Commun.* **2018**, *50*, 22–26.
52. Santos, G.O.S.; Gonzaga, I.M.D.; Eguiluz, K.I.B.; Salazar-Banda, G.R.; Saez, C.; Rodrigo, M.A. Improving biodegradability of clopyralid wastes by photoelectrolysis: The role of the anode material. *J. Electroanal. Chem.* **2020**, *864*, 114084. [CrossRef]
53. Chiang, L.C.; Chang, J.E.; Wen, T.C. Indirect oxidation effect in electrochemical oxidation treatment of landfill leachate. *Water Res.* **1995**, *29*, 671–678. [CrossRef]
54. Baker, J.R.; Milke, M.W.; Mihelcic, J.R. Relationship between chemical and theoretical oxygen demand for specific classes of organic chemicals. *Water Res.* **1999**, *33*, 327–334. [CrossRef]
55. Stoddart, A.K.; Gagnon, G.A. Application of photoelectrochemical chemical oxygen demand to drinking water. *J. Am. Water Works Assoc.* **2014**, *106*, E383–E390. [CrossRef]
56. He, W.; Chen, S.; Liu, X.; Chen, J. Water quality monitoring in a slightly-polluted inland water body through remote sensing—Case study of the Guanting Reservoir in Beijing, China. *Front. Environ. Sci. Eng. China* **2008**, *2*, 163–171. [CrossRef]
57. Melin, E.S.; Ødegaard, H. Biofiltration of ozonated humic water in expanded clay aggregate filters. *Water Sci. Technol.* **1999**, *40*, 165–172. [CrossRef]
58. Särkkä, H.; Vepsäläinen, M.; Pulliainen, M.; Sillanpää, M. Electrochemical inactivation of paper mill bacteria with mixed metal oxide electrode. *J. Hazard. Mater.* **2008**, *156*, 208–213. [CrossRef]

59. Zhou, S.; Bu, L.; Yu, Y.; Zou, X.; Zhang, Y. A comparative study of microcystin-LR degradation by electrogenerated oxidants at BDD and MMO anodes. *Chemosphere* **2016**, *165*, 381–387. [CrossRef] [PubMed]
60. Edzwald, J.K.; Tobiason, J.E. Enhanced coagulation: US requirements and a broader view. *Water Sci. Technol.* **1999**, *40*, 63–70. [CrossRef]
61. Jung, C.W.; Son, H.J. The relationship between disinfection by-products formation and characteristics of natural organic matter in raw water. *Korean J. Chem. Eng.* **2008**, *25*, 714–720. [CrossRef]
62. Nkambule, T.I.; Kuvarega, A.T.; Krause, R.W.M.; Haarhoff, J.; Mamba, B.B. Synthesis and characterisation of Pd-modified N-doped TiO2 for photocatalytic degradation of natural organic matter (NOM) fractions. *Environ. Sci. Pollut. Res.* **2012**, *19*, 4120–4132. [CrossRef]
63. Wong, H.; Mok, K.M.; Fan, X.J. Natural organic matter and formation of trihalomethanes in two water treatment processes. *Desalination* **2007**, *210*, 44–51. [CrossRef]
64. Edzwald, J.K.; Becker, W.C.; Wattier, K.L. Surrogate parameters for monitoring organic matter and THM precursors. *J.-Am. Water Work. Assoc.* **1985**, *77*, 122–132. [CrossRef]
65. Dbira, S.; Bensalah, N.; Ahmad, M.I.; Bedoui, A. Electrochemical Oxidation/Disinfection of Urine Wastewaters with Different Anode Materials. *Materials* **2019**, *12*, 1254. [CrossRef]
66. Moratalla, Á.; Lacasa, E.; Cañizares, P.; Rodrigo, M.A.; Sáez, C. Electro-Fenton-Based Technologies for Selectively Degrading Antibiotics in Aqueous Media. *Catalysts* **2022**, *12*, 602. [CrossRef]
67. Jiang, Y.; Zhao, H.; Liang, J.; Yue, L.; Li, T.; Luo, Y.; Liu, Q.; Lu, S.; Asiri, A.M.; Gong, Z.; et al. Anodic oxidation for the degradation of organic pollutants: Anode materials, operating conditions and mechanisms. A mini review. *Electrochem. Commun.* **2021**, *123*, 106912. [CrossRef]